

Dependence of the High-Field Flux-Flow Resistivity upon the Sample Demagnetization Factor in Type-II Superconductors

G. E. Kuhl and M. C. Ohmer

Air Force Materials Laboratory, Wright-Patterson Air Force Base, Ohio 45433

(Received 19 February 1970)

We have experimentally determined the orientational dependence of the flux-flow resistivity ρ_F due to the sample geometry in several type-II Pb-Tl alloys at 4.2°K. The demagnetization factors of the samples were varied from 0.1 to 0.9 by rotating the magnetic field in relation to the sample plane, always perpendicular to the sample current. The flux-flow resistivity increased with decreasing demagnetization factor for $\text{Pb}_{0.971}\text{Tl}_{0.029}$ and $\text{Pb}_{0.95}\text{Tl}_{0.05}$ samples with κ values of 0.97 and 1.28, respectively. The flux-flow resistivity for a $\text{Pb}_{0.60}\text{Tl}_{0.40}$ sample with a κ of 4.90 was essentially independent of the demagnetization factor. The experimental results were found to agree with the theoretical demagnetization-factor dependence of ρ_F predicted by Caroli and Maki and by Cape and Zimmerman.

INTRODUCTION

The flux-flow resistivity ρ_F for type-II superconductors has been the topic of numerous theoretical and experimental investigations in recent years.¹⁻⁷ Of particular applicability to the analysis of the experimental results of high-field flux-flow measurements to be presented in this paper are the papers of Schmid² and Caroli and Maki³ which contain theoretical expressions for the flux-flow resistivity near H_{c2} . For the dirty-limit situation, they found that ρ_F/ρ_N at H_{c2} can be expressed as

$$\rho_F/\rho_N = 1 + [4\pi M] [4\kappa_1^2(0)]/H_{c2}(t). \quad (1)$$

Cape and Zimmerman⁸ had earlier considered the effects of nonzero demagnetization factor n upon the magnetization of ellipsoidal superconductors. Their result for the external field H parallel to a principal axis is expressed as

$$4\pi M = [H - H_{c2}(t)] / \{1.16[2\kappa_2^2(t) - 1] + n\}. \quad (2)$$

In these expressions, κ_1 and κ_2 are the Ginzburg-Landau parameters as defined in Maki's earlier papers.⁵ Combining this result with that of Caroli and Maki, ρ_F/ρ_N at H_{c2} can be expressed as

$$\rho_F/\rho_N = 1 - \frac{4\kappa_1^2(0)[1 - H/H_{c2}(t)]}{1.16[2\kappa_2^2(t) - 1] + n}. \quad (3)$$

For comparison of experimental and theoretical results it is more convenient to work with the dimensionless ratio α defined as

$$\alpha = \left[H \frac{d}{dH} \frac{\rho_F}{\rho_N} \right]_{(H=H_{c2})}. \quad (4)$$

Using Eq. (3), the value of α is

$$\alpha(n) = 4\kappa_1^2(0) / \{1.16[2\kappa_2^2(t) - 1] + n\}. \quad (5)$$

We have measured the flux-flow resistivities of

a number of alloys to obtain the experimental orientational dependence of ρ_F . We have employed techniques very similar to those of Axt and Joiner⁶ for these measurements. The κ values of the alloy samples range from small values (≈ 1) to relatively large values (≈ 5). The results of these experimental measurements are presented in this paper and are compared with the theoretical results predicted by Eq. (5).

SAMPLE PREPARATION AND EXPERIMENTAL PROCEDURES

The materials chosen for this study of the dependence of α upon the orientation-dependent demagnetization factor $n(\theta)$ were Pb-Tl alloys with Tl concentrations of 2.9, 5.0, and 40.0 at.%. The Pb-Tl alloy system was chosen because it is known to possess relatively low critical currents when properly treated, thereby minimizing the adverse effects of sample heating, and also because several detailed studies of the temperature dependences of κ_1 and κ_2 are available from previous work of other experimenters.^{9,10}

The alloy ingots were obtained by melting carefully weighed mixtures of Pb and Tl in Pyrex tubes under a vacuum of 10^{-7} Torr for periods of 24 h or longer. The molten mixture was vigorously stirred by continuous vibration and was then rapidly air quenched to insure sample homogeneity. The starting materials were Cominco 69-Grade Pb (shot) and Tl (ingot). Alloy cylinders approximately 1.0 mm in diameter were cast from the ingots in capillary tubes under identical conditions.

Individual samples were prepared by pressing short sections of the alloy cylinders between glass microscope slides to obtain thickness-to-width ratios t/w of approximately 0.1. The sample retained its mirrorlike finish throughout this pro-

cess and remained relatively untarnished before being given a thick (greater than 1000 Å) copper coating to reduce surface superconductivity. This coating was applied by vapor deposition of high-purity copper in a vacuum of 10^{-6} Torr. These coated samples were then annealed at 300 °C for several days. The shape of the resulting samples was that of a rectangular slab with rounded edges. This shape approximates an elliptical right cylinder with a high degree of ellipticity. In this case, the demagnetization factors of elliptical right cylinders are a good approximation to the demagnetization factors of our samples.

The sample was then clamped in a standard four-probe device constructed of Teflon and low-resistivity copper. The sample was clamped between large copper current contacts at the ends of the holder and copper voltage contacts 0.5 in. apart in the central region of the sample. The sample holder was then immersed in liquid helium and all measurements were conducted at 4.2 °K. The orientation of the sample is shown in Fig. 1. The current I is always perpendicular to the applied field H and the angle θ between the sample plane and H , and hence the demagnetization factor $n(\theta)$, can be varied by rotating the field with respect to the sample. For $0^\circ \leq \theta \leq 90^\circ$, $n(\theta)$ varies from approximately 0.1 to 0.9 for our samples.

Flux-flow voltages were measured and amplified by a Keithley model 148 nanovoltmeter and the amplified voltage was recorded on the Y axis of a Moseley model 7000AR X-Y recorder. The sample voltage levels ranged from 0.5 to 1.0 mV. The current was provided by a Hewlett-Packard model 6269A dc power supply. The voltage signal for the X axis of the recorder was provided by the voltage drop across a Weston precision shunt in series with the sample. Flux-flow characteristics were recorded at 10-G intervals below H_{c2} for each of a

number of orientations in the case of the 2.9- and 5.0-at.% Tl samples, and at 50-G intervals in the 40.0-at.% Tl sample. The flux-flow resistivities were determined from the slopes of the linear portions of the flux-flow characteristics.

SAMPLE PARAMETERS

The relevant parameters of our samples and those quantities appearing in calculations of $\alpha(n)$ using the theory of Caroli and Maki³ are listed in Table I. The values of κ shown in columns (b) and (c) are the κ values of our samples as determined from two different methods. The first κ value is that found from the normal-state resistivity ρ_N and the Gorkov-Goodman equation.¹¹ The second κ value is that determined from the experimental value of H_{c2} .

In order to compare our experimental results with those calculated using the results of Caroli and Maki, it is necessary to know κ and the temperature dependence $\kappa_1^*(t)$ and $\kappa_2^*(t)$ which can be defined as

$$\kappa_{1,2}^*(t) = \kappa_{1,2}(t) / \kappa. \quad (6)$$

For good numerical agreement between theory and experiment these quantities must be accurately known. A number^{5,12-14} of theoretical calculations of $\kappa_1^*(t)$ have been made, all with essentially the same results. Eilenberger¹⁴ has made the most comprehensive calculations, including the effects of sample purity for various combinations of s -wave and p -wave scattering of the impurities. His results for $\kappa_1^*(t)$ in the case of s -wave scattering will be used since the experimental results of other workers^{9,10} indicate that this situation is very nearly correct for the Pb-Tl alloy system. The κ values measured for our samples indicate that they are sufficiently "dirty"¹⁴ for the valid application of the dirty-limit result for $\alpha(n)$ expressed by Eq. (6).

It is apparent that the values of $\kappa_1^*(0)$ in Table I are very different from the dirty-limit value (≈ 1.2) predicted by Eilenberger and others. Their results must be modified to account for the non-BCS behavior of real superconductors.¹⁵ In this case $\kappa_1^*(0) \approx 1.47$ for dirty Pb superconductors. Experimental values of $\kappa_1^*(0)$ are in excellent agreement with this value.^{9,10}

The temperature dependence $\kappa_2^*(t)$ is not well established experimentally. Theoretically, the work of Eilenberger shows that $\kappa_2^*(t) > \kappa_1^*(t)$ for a given purity, and that the difference between the two decreases with decreasing purity. These results were found to be qualitatively correct in Nb by Finnemore *et al.*¹⁶ However, an opposite result was found in the Pb-Tl alloy system by Sekula, and Kernohan. In their alloys (concentrations of

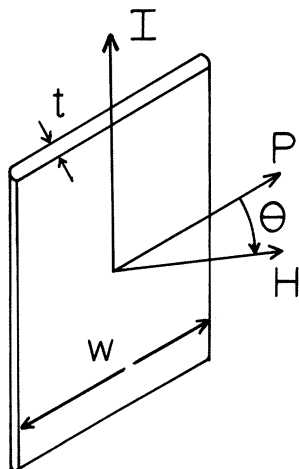


FIG. 1. Sample geometry. Sample shape approximates highly elliptic right cylinder. Field H is always perpendicular to the current I . Angle θ between H and the sample plane P was varied by rotating the magnet with respect to the sample.

TABLE I. Sample parameters. (b) κ determined from measurement of ρ_N ; (c) κ determined from measurements of H_{c2} (4.2°K); (d) temperature dependence of κ_1 at $T=0$ °K; (e) temperature dependence of κ_2 at $T=4.2$ °K taken from the paper of Bon Mardion *et al.*; (f) the same quantity as determined by Sekula and Kernohan; (g) thickness-to-width ratios; (h) sample demagnetization factor for H perpendicular to sample plane; and (i) demagnetization factor for H parallel to sample plane.

(a) Composition (at. % Tl)	(b) κ	(c) κ	(d) $\kappa_1^*(0)$	(e) $\kappa_2^*(t)$	(f) $\kappa_2^*(t)$	(g) t/w	(h) $n(90^\circ)$	(i) $n(0^\circ)$
2.9	0.97	0.99	1.480	1.15	1.21	0.101	0.91	0.09
5.0	1.28	1.24	1.474	1.18	1.24	0.103	0.91	0.09
40.0	4.90	5.25	1.464	1.20	1.34	0.144	0.87	0.13

Tl ranging from 4 to 27 at.%, they found $\kappa_2^*(t) > \kappa_1^*(t)$ as predicted, but the difference between the two increased as purity decreased. Similar results were observed by Bon Mardion *et al.*, but in their alloys (concentrations of Tl ranging from 1.2 to 75-at.% Tl) they observed a less pronounced increase in the difference between $\kappa_2(t)$ and $\kappa_1(t)$ as purity decreases. Since $\kappa_2^*(t)$ has not been established definitely, values of $\kappa_2^*(t)$ for $T=4.2$ °K have been estimated from the results of both Mardion *et al.* and Sekula and Kernohan and are included in Table I. Both sets of $\kappa_2^*(t)$ will be used in calculating $\alpha(n)$.

The remaining columns of Table I represent the physical dimensions of the individual samples. Since the sample shape approximated an elliptical right cylinder of a high degree of ellipticity, the values of the demagnetization factor $n(90^\circ)$, for H perpendicular to the plane of the large sample face, and $n(0^\circ)$ for H parallel to the plane of the large sample face, can be approximated by the expressions for these quantities in the case of elliptical right cylinders,¹⁷

$$n(90^\circ) = (1 + t/w)^{-1}, \quad (7a)$$

$$n(0^\circ) = 1 + w/t)^{-1}. \quad (7b)$$

The values of $n(\theta)$ at intermediate angles lie between these extremes.

EXPERIMENTAL RESULTS

The experimental results of our measurements of ρ_F (normalized by dividing these measured quantities by ρ_N) are presented in Figs. 2-4 for the cases of the 2.9-, 5.0-, and 40.0-at.% Tl samples, respectively. The range of magnetic field over which we observed a linear dependence of $\ln(\rho_F/\rho_N)$ in field is represented by the unbroken straight lines. These lines are those fitted to the data points by computer. The data points shown in these figures are only a few of those actually measured, the remainder having been neglected for reasons of clarity. The linear dependence generally began at fields somewhat lower than H_{c2} . In

the field region just below H_{c2} the experimental values of ρ_F did not follow this dependence, the values generally lying above the straight line in the 40.0-at.% Tl case, and below the straight line in the other cases. For all three alloy compositions the data points in this region varied erratically with field and have not been considered in the determination of the fitted straight line. It is thought that

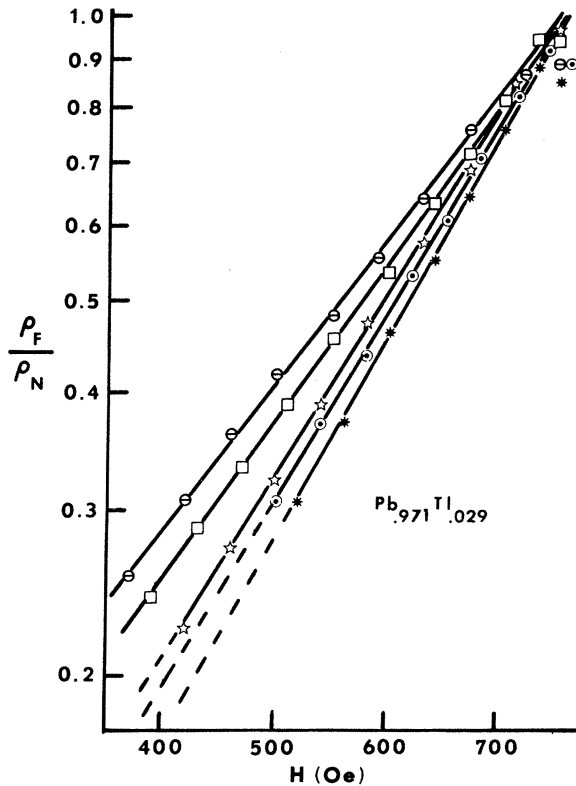


FIG. 2. Field dependence of normalized flux-flow resistivity in a $\text{Pb}_{0.971}\text{Tl}_{0.029}$ sample. Solid lines represent the least-squares fit to data points. Lines and data points in order of increasing slope represent data for the $\theta=90^\circ, 45^\circ, 30^\circ, 10^\circ$, and 5° orientations, respectively.

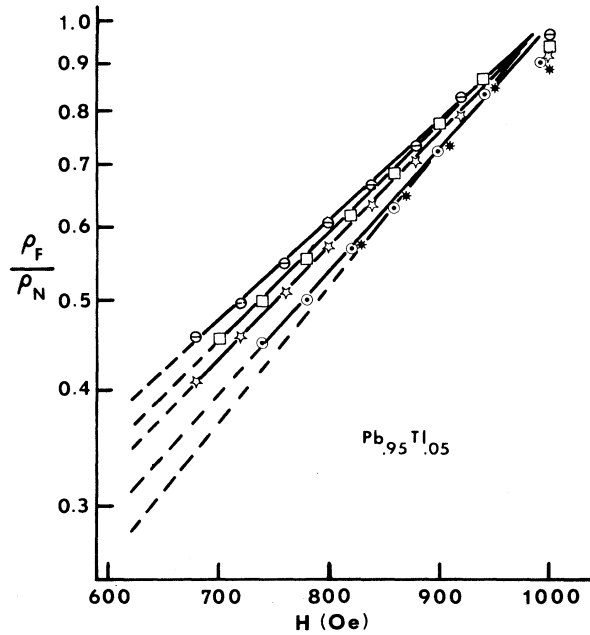


FIG. 3. Field dependence of normalized flux-flow resistivity in $\text{Pb}_{0.95}\text{Tl}_{0.05}$ sample. In order of increasing slope data points and computer fitted lines represent $\theta = 90^\circ, 45^\circ, 30^\circ, 10^\circ$, and 5° , respectively.

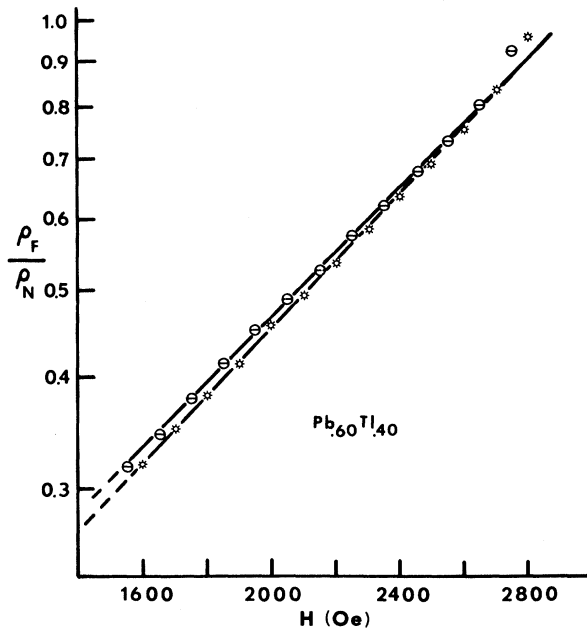


FIG. 4. Field dependence of normalized flux-flow resistivity in a $\text{Pb}_{0.60}\text{Tl}_{0.40}$ sample. Upper data points and computer fitted line represent the $\theta = 90^\circ$ orientation, lower ones are for the $\theta = 0^\circ$ orientation. Intermediate angles are not represented for reasons of clarity.

the erratic behavior of the data points in this region is due to heating effects in the samples. At lower fields, $\ln(\rho_F/\rho_N)$ is no longer linear in H , and the experimental values were found to lie below the straight line in agreement with the experimental work of others.^{6,7} In addition, the large currents required in the lower-field regions for cases of small κ created heating problems in the lower-Tl-concentration alloys which limited the field range of reliable data. Linear flux-flow characteristics

could not be obtained for the parallel ($\theta = 0^\circ$) orientation in the 2.9- and 5.0-at.% Tl samples. Only the extreme cases $n(\theta) = n(90^\circ)$, $n(0^\circ)$ are represented in Fig. 4 since the values of $\alpha(n)$ for the 40.0-at.% Tl alloy do not vary to any great extent for the entire range of $n(\theta)$.

The values of $\alpha(n)$ calculated from these slopes are listed in Table II together with values of $\alpha(n)$ calculated from Eq. (5). The first value listed for

TABLE II. Experimental and theoretical values of $\alpha(n)$. The first quantity in each series of three values for each sample and orientation is the experimental value of α ; the second quantity is the theoretical value of α using the values of κ_2^* (4.2°K) measured by Bon Mardion *et al.*; the third quantity is the theoretical value of α found using the experimental results of Sekula and Kernohan for κ_2^* (4.2°K).

(a) Composition (at. % Tl)	(b) $\alpha(\theta = 90^\circ)$	(c) $\alpha(\theta = 45^\circ)$	(d) $\alpha(\theta = 30^\circ)$	(e) $\alpha(\theta = 10^\circ)$	(f) $\alpha(\theta = 5^\circ)$	(g) $\alpha(\theta = 0^\circ)$
2.9	3.16	3.43	4.01	4.15	4.41	...
	3.12	3.48	3.76	4.31	4.45	4.52
	2.79	3.07	3.30	3.71	3.81	3.87
5.0	2.76	2.97	3.01	3.32	3.70	...
	2.83	2.99	3.10	3.30	3.35	3.37
	2.55	2.68	2.77	2.93	2.97	2.99
40.0	2.54	2.53	2.60	2.58
	2.58	2.60
	2.06	2.08

each orientation and each alloy is the experimental values from the slope of the computer-fitted straight line. The second value is the value $\alpha(n)$ calculated from the theoretical result of Caroli and Maki, making use of the experimental results for $\kappa_2^*(t)$ found by Bon Mardion *et al.* The third value is also calculated from Caroli and Maki's results, but $\kappa_2^*(t)$ is that estimated from the results of Sekula and Kernohan.

The results shown in this table indicate good qualitative agreement with the theoretical demagnetization factor dependence of ρ_F/ρ_N . The experimental values of $\alpha(n)$ increase as n decreases. The quantitative agreement of the experimental $\alpha(n)$ with those calculated from Eq. (6) is only fair. The qualitative agreement is emphasized in Fig. 5 in which the solid lines represent the theory of Caroli and Maki using the experimental results for $\kappa_2^*(t)$ as found by Bon Mardion *et al.* The data points shown indicate a monotonic increase in $\alpha(n)$ as n decreases for all three alloy concentrations (the scatter in the 40.0-at.% Tl data is well within the range of experimental accuracy). The increase in $\alpha(n)$ also becomes less pronounced as concentration (and κ) increases, becoming almost nonexistent in the 40.0-at.% Tl ($\kappa \approx 5$) case.

DISCUSSION

The flux-flow resistivity was found to be logarithmic in magnetic field over a wide range of field. This result is in agreement with the results of Axt and Joiner⁶ and Usui *et al.*⁷ This exponential dependence in H of ρ_F/ρ_N , which can be expressed as $\exp\alpha(H/H_{c2} - 1)$, is not in disagreement with the linear relationship of Eq. (3) predicted by Caroli-Maki theory. For $H \approx H_{c2}$, the first two terms of the series expansion of this exponential term yield Eq. (3). Since Eq. (3) is strictly valid only in the field region just below H_{c2} , the experimental and theoretical field dependence of ρ_F/ρ_N near H_{c2} are in agreement. The fact that ρ_F varies exponentially with field below H_{c2} greatly simplifies the experimental determination of α . In the immediate vicinity of H_{c2} it is experimentally difficult to obtain reliable flux-flow data because of large heating effects. However, because of the exponential magnetic field dependence of ρ_F over a large field range below H_{c2} , α can be determined from values of ρ_F measured at lower fields in which sample heating is no longer a problem.

The experimental results shown in Figs. 2-5 and tabulated in Table II clearly establish the qualitative agreement between the experimental results and the theoretical dependence of ρ_F/ρ_N upon the demagnetization factor. The quantitative agreement, although quite good for the values of $\kappa_1^*(0)$ and $\kappa_2^*(t)$ which we have used, cannot be completely

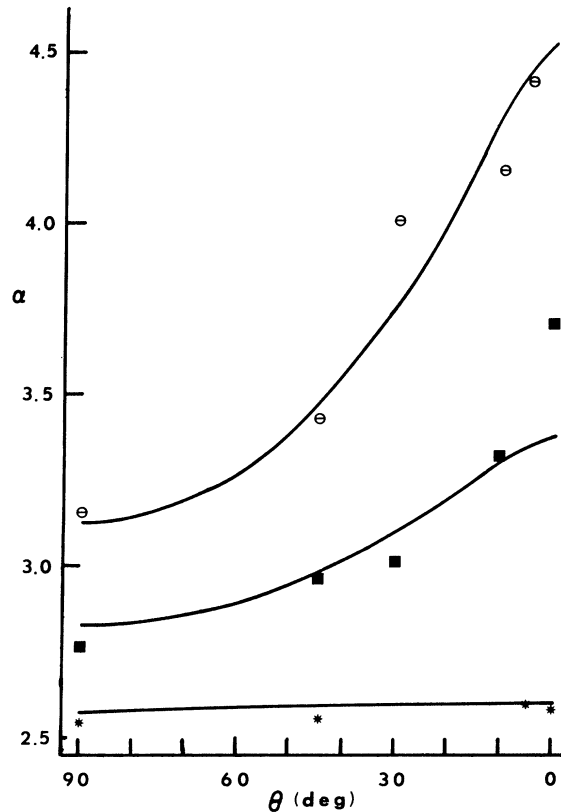


FIG. 5. Angular dependence of the quantity α . Upper curve represents data taken on $\text{Pb}_{0.971}\text{Tl}_{0.029}$ sample; intermediate curve represents data from $\text{Pb}_{0.95}\text{Tl}_{0.05}$ sample; and lower curve is for $\text{Pb}_{0.60}\text{Tl}_{0.40}$ sample. Data points are found from measured values; solid lines are calculated from Eq. (5) using values of $\kappa_1(0)$ and $\kappa_2(t)$ estimated from the previous work of Bon Mardion *et al.* Quantitative agreement is only fair but it can be observed that α increases with decreasing θ (and n). Values of α are smaller and the increase in α as n decreases is less pronounced as κ (and increasing Tl concentration) increases.

established. This could be done only if experimental values of $\kappa_1^*(t)$ and $\kappa_2^*(t)$ for each of our alloy samples were measured directly, and, in addition, detailed calculations of $n(\theta)$ made. The results of Bon Mardion *et al.*, and those of Sekula and Kernohan, while in qualitative agreement, provide significantly different results for $\alpha(n)$ as calculated from Eq. (5). Although the results of measurement of $\kappa_2^*(t)$ by Bon Mardion *et al.* provide much better theoretical agreement without experimental data, it is impossible at this time to determine which set of data for $\kappa_2^*(t)$ is correct. It is for this reason that results of this measurement by each group have been included in this paper. For the purposes of this paper detailed calculations of

$n(\theta)$ are not warranted and estimates of $n(\theta)$ based on the values of $n(0^\circ)$ and $n(90^\circ)$ for right elliptical cylinders are sufficiently accurate.

The observed variation of $\alpha(n)$ for the 2.9-at.% Tl alloy as $n(\theta)$ varied from the $n(90^\circ)$ to $n(5^\circ)$ was approximately 40%, very nearly equal to that predicted by Eq. (6). Even greater variation of $\alpha(n)$ is predicted for smaller values of κ . However, attempts to measure the flux-flow resistivities in alloys with concentrations of 2.0- and 2.6-at.% Tl, κ values of 0.75 and 0.88, respectively, were unsuccessful due to nonlinearity of the flux-flow characteristics at lower values of θ . These nonlinearities were due to higher critical currents in these lower-concentration alloys. In view of the precautions taken to assure lower current values in our samples it appears to be highly unlikely that reliable flux-flow data could be obtained at all angles at lower values of κ in this alloy system.

The experimental value of $\alpha(n)$ for $\theta = 90^\circ$ can be compared to that measured by Axt and Joiner for two of the concentrations studied. In their 40-at.% Tl sample, their value of α ($T = 4.2^\circ\text{K}$), which was measured at an orientation equivalent to our $\theta = 90^\circ$ orientation, is in excellent agreement without value. For the other alloy composition common to both studies, 5.0-at.% Tl, the agreement is not good, the value of Axt and Joiner being some 15% lower than that which we observed. The reason for this difference, which is outside the range of experimental error, is unknown.

Cape and Silvera⁴ investigated the resistivity of a single In-Bi alloy sample as a function of field for two sample orientations in which the demagnetization factors were approximately 0.02 and 0.98. They observed significantly different α 's for the two orientations and found that their experimental values of α agreed, to within 10%, with those calculated from the theory of Caroli and Maki. However, Cape and Silvera employed a different experimental procedure which involved the use of an ac magnetic field to depin the fluxoids. The influence of an ac magnetic field upon the fluxoids in the mixed state of type-II superconductors is not as yet completely understood. Additionally, α must be determined from the slope of the linear portion of the R -versus- H curve by this method. The field range over which R is linear in H is very small in

view of experimental results.^{6,7} In all probability, the linear relationship between R and H holds only for fields very near H_{c2} so the determination of α by this method is less accurate than by the method employed in this paper.

An earlier paper by Swartz and Hart¹⁸ studied flux-flow in a $\text{Pb}_{0.95}\text{Tl}_{0.05}$ unplated sample as part of an extensive study of surface effects in the mixed superconducting state. They measured ρ_F/ρ_N for several sample orientations corresponding to our $\theta = 5^\circ$, 15° , and 90° orientations. As in our study, they found it impossible to obtain reliable flux-flow characteristics for the $\theta = 0^\circ$ orientation, a situation which is understandable since their sample was uncoated. They observed ρ_F/ρ_N for a given field value to decrease with angle as we have observed. However, from the limited amount of data which they present, it is impossible to determine if the slope of ρ_F/ρ_N is actually increasing with decreasing angle as we have observed. They interpret their experimental results in terms of the surface retarding the motion of the fluxoids through the sample at the low-angle orientations, a situation which is highly unlikely in terms of present knowledge of the dissipative processes in type-II superconductors. A more likely explanation of their experimental results is that their flux-flow resistivities were affected by the demagnetization factor of their samples, as were ours.

In summary, we can state that direct measurements of the flux-flow resistivities support the theoretical result obtained from Caroli and Maki and Cape and Zimmerman for the dependence of the flux-flow resistivity upon the demagnetization factor of the sample. The experimental values of $\alpha(n)$ vary with n in a manner which is in good qualitative agreement with the theoretical results. Quantitative agreement can be judged only fair since several of the quantities in the expression for α are known only approximately.

ACKNOWLEDGMENTS

We would like to thank Dr. C. J. Axt and Dr. W. C. H. Joiner for several helpful discussions of their experimental results. In addition, we would like to thank A. Biermann and R. A. Winn for their help in sample preparation.

¹Y. B. Kim, C. F. Hempstead, and A. R. Strnad, Phys. Rev. **139**, A1163 (1965); A. R. Strnad, C. F. Hempstead, and Y. B. Kim, Phys. Rev. Letters **13**, 794 (1964); J. Bardeen and M. J. Stephen, Phys. Rev. **140**, A1197 (1965); W. C. H. Joiner and G. E. Kuhl, *ibid.* **168**, 413 (1968).

²A. Schmid, Phys. Kondensierten Materie **5**, 302 (1966).

³C. Caroli and K. Maki, Phys. Rev. **164**, 591 (1967).

⁴J. A. Cape and I. F. Silvera, Phys. Rev. Letters **20**, 326 (1968).

⁵K. Maki, Physics **1**, 21 (1964); **1**, 127 (1964).

⁶C. J. Axt and W. C. H. Joiner, Phys. Rev. **171**, 461 (1968).

⁷N. Usui, T. Ogasawara, K. Yasukochi, and S. Tomoda, J. Phys. Soc. Japan **27**, 574 (1969).

- ⁸J. A. Cape and J. M. Zimmerman, Phys. Rev. **153**, 416 (1967).
⁹S. T. Sekula and R. H. Kernohan, J. Phys. Chem. Solids **27**, 1863 (1966).
¹⁰G. Bon Mardion, B. B. Goodman, and A. Lacaze, J. Phys. Chem. Solids **26**, 1143 (1965).
¹¹B. B. Goodman, IBM J. Res. Develop. **6**, 62 (1962).
¹²C. Caroli, M. Cyrot, and P. G. de Gennes, Solid State Commun. **4**, 17 (1966).
¹³E. Helfand and N. R. Werthamer, Phys. Rev. **147**, 288 (1966).
¹⁴G. Eilenberger, Phys. Rev. **153**, 584 (1967).
¹⁵G. Cody, in Proceedings of the 1968 Summer Study of Superconducting Devices and Accelerators, Brookhaven National Laboratory, Part II, p. 406 (unpublished).
¹⁶D. K. Finnemore, T. F. Stroudsberg, and C. A. Swenson, Phys. Rev. **149**, 231 (1966).
¹⁷W. F. Brown, Jr., *Magnetostatic Principles in Ferromagnetism* (North-Holland, Amsterdam, 1962), Appendix, p. 187.
¹⁸P. S. Swartz and H. R. Hart, Jr., Phys. Rev. **137**, A818 (1965).

Collective Excitation Spectroscopy in Superconductor-Semiconductor Tunnel Junctions*

C. B. Duke

*Department of Physics, Materials Research Laboratory, and Coordinated Science Laboratory,
University of Illinois, Urbana, Illinois 61801*

and

G. G. Kleiman

Department of Physics and Materials Research Laboratory, University of Illinois, Urbana, Illinois 61801
(Received 19 December 1969)

The transfer-Hamiltonian description of the influence of electron-boson interactions on the electrical characteristics of metal-semiconductor tunnel junctions is extended by considering the combined effects of electrode self-energy phenomena and boson-assisted tunneling. The current associated with these processes is evaluated for superconducting metal electrodes described by the pairing model as well as for normal metal electrodes. Numerical evaluations of the conductance are made using models and parameters appropriate for the description of the influence of electron (hole) interactions with optical phonons (energy $\cong \hbar \omega_0$) on the tunneling characteristics of metal contacts on boron-doped silicon.

I. INTRODUCTION

In the past few years, the transfer-Hamiltonian description^{1,2} of electron tunneling in solids has been extended³⁻⁹ and shown to be capable of describing qualitatively the various types of many-body effects which have been observed in tunnel junctions⁶ (with the sole exception of tunneling through real intermediate states^{6,10,11}). In this paper we report two new extensions of this description: the simultaneous consideration both in inelastic tunneling and of electrode self-energy effects, and the study of these phenomena in metal-semiconductor tunnel junctions in which the metal electrode is a superconductor.

To understand the motivation for the importance of these extensions, let us recall some of the main features of the transfer-Hamiltonian description of the influence of electron-phonon coupling in the semiconductor on the conductance characteristics of metal-semiconductor tunnel junctions. The essence of this description is that once a set of basis states for the "electrode" wave function

have been selected, the junction Hamiltonian can be written formally as

$$\mathcal{H} = \mathcal{H}_L + \mathcal{H}_R + \mathcal{H}_T, \quad (1.1)$$

in which \mathcal{H}_L and \mathcal{H}_R describe matrix elements between states in the left- and right-hand electrodes, respectively, and \mathcal{H}_T describes matrix elements which transfer an electron from one electrode to the other. The tunneling current is evaluated by a straightforward linear response analysis in which \mathcal{H}_T is treated as the "external" source.⁶ This analysis permits us to introduce a diagrammatic description of the tunnel current⁶ analogous to that of the linear-response theory of electrical conductivity.^{12,13} The diagrammatic analysis is developed in detail in Refs. 4 and 6. Therefore, in Fig. 1 we merely present some of the relevant diagrams for the current. Figure 1(a) specifies the elastic current which, if an independent electron model is used to describe both metal and semiconductor, reduces to the ordinary one-electron current through a potential barrier.⁶ Davis and Duke^{7,14} extended the analysis of this diagram